Different Phases in Multilane Traffic Based on Generalized Nagel-Schreckenberg Model

Fan Ningyue, Zhang Chengyan, and Zhang Yutai
Department of Physics, Fudan University, Shanghai 200433, China

Studying road traffic with CA models has long been of interest in the field of statistical mechanics. Previous models have considered either multilane traffic or inhomogeneous cars. However, very few model has combined them together to give a more comprehensive picture of traffic. Thus, this study sets out to explore a generalized NaSch model with both two factors. The aim of this study is to investigate the macroscopic properties of the generalized model. Three phases, the FF phase, the BEC phase and the HC phase, are found. Different macroscopic quantities, including entropy, vacancy or platoon length and degeneracy, are defined and investigated in different phases.

I. INTRODUCTION

Modeling traffic flow has been of considerable interest to physicists due to its wide applications [1]. Since cars can be seen as particle systems far from equilibrium [2], statistical approaches can be utilized to understand traffic flow.

Current models for single-lane traffic flow can be categorized into 3 classes: macro-, meso- and microscopic models (see [1, 2] for an overview, or [3] , a more recent one). A comprehensive review of different models is out of the scope of our research, but it's necessary to mention some of the representative and important models. In macroscopic models, traffic flow is viewed as continuum, analogous to the hydrodynamics of compressible fluid. Equation of continuity [4] and Navier-Stokes-like equation for traffic flow [5] have been formulated. However, macroscopic models cannot depict the behavior of individual vehicles. Thus it not easy to approach with statistical mechanics. Mesoscopic models are analogous to kinetic theories of gases, and focus on the probability distribution of cars. Boltzmann-like equation has been established [6]. On the other hand, in microscopic models, each individual car is modeled. Every car is thought to be adjusting its speed based on local situation, such as speed difference and distance headway (distance between two cars), which can be seen as a generalized Newton's equation for cars [1]. Typical models are follow-the-leader model [7] and optimal velocity model [8].

However, obtaining analytical solutions is not easy and thus numerical simulations are often utilized. Therefore, one kind of microscopic models, cellular automata (CA) models, have attracted much attention [9] due to its higher simulation efficiency than other models. In CA models, space and time are discretized. The road is represented by a 1-dimensional lattice consisting of cells. The updating of cars on the roads follow certain rules. As CA models are discretized in nature, statistical mechanical methods can be easily applied. A specific single-lane CA model, the Nagel-Shreckenberg (NaSch) model [10], is able to reproduce essential phenomena in traffic flow while remain simple [2]. Therefore, much research has been carried out to explore the behavior of this model (see section 8 of [2] for an overview). It bears much similarity to the asymmetric simple exclusion process (ASEP) [2]. In this study, the NaSch model will be employed because of its simple yet rather complete description of traffic flow.

Various phenomena and properties of traffic have been widely studied based on different models and theories. The original single-lane NaSch model is generalized to include multilane traffic [11–13], in which the mean field approach has also been applied recently [14, 15]. Another generalization is to consider the difference between cars: parameters such as maximal speed of cars can be designed to follow a probability distribution instead of taking a universal value. In these models, "fast cars" will queue up behind a "slow car" and form a platoon[16]. This phenomenon is analogous to Bose-Einstein Condensation (BEC) [2]. Such analogy has been made precise in ASEP [17, 18], but not in the NaSch model yet. These generalizations are essential parts of the real traffic and is necessary for traffic models.

However, in real traffic, lane changing cannot be omitted when a Bose-Einstein-like condensation happens due to a slow car. But to the best of our knowledge, this BEC-like phenomenon has not been studied in a multilane model. Therefore, this study explores a modified NaSch model which can describe the lane-changing behavious in multilane traffic better. This study attempts to study the macroscopic properties of this model. Different phases are found and macroscopic variables featuring different phases are defined and studied.

The following content is divided into five sections. After the introduction, the model is defined in the section II. To yield an overall understanding, a qualitative description and the phase diagram of the model is given in section III and IV. Then, the macroscopic features of the FF phase and the BEC phase are respectively discussed in section V and VI.

II. MODEL

The model suggested by Nagel and Schreckenberg (NaSch) [10, 19] is a CA model where N particles or cars move on a lane with l_0 lattices. We will take periodic boundary condition (PBC) here and after. The density of the road is defined by $\rho = N/l_0$. Each cell is labeled by an index $1, 2, \ldots, l_0$ to represent its position. The position of car k is defined as the index of the cell occupied by the car, denoted by r_k. Then the *headway* of car k is defined by $d_k = r_l - r_k$, where car l is the car immediately in front of car k. (The number of empty cells beyond a car is $d_k - 1$.) Note that $\sum_{k=1}^{N} d_k = l_0$ due to PBC. Each car $1 \leq k \leq N$ possesses an integer speed v_k such that $0 \leq v_k \leq v_{\text{max}}$, where v_{max} is a maximum speed up to choice. At each time step, four rules are applied to update the state of all the cars. Time t is defined as the number of steps after the

initial state $t = 0$. The rules applied to all cars $1 \leq k \leq N$ at time $t \leq 0$ are then given by:

1. Acceleration. The speed increases by one if smaller then the maximum speed. Otherwise it keeps the same, i.e., $v'_k(t+1) = \min[v_k(t)+1, v_{\max}]$.
2. Deceleration (to avoid bumping into other vehicles). The speed decreases to $d_k - 1$ if its larger then it. Otherwise the speed keeps the same, i.e., $v''_k(t+1) = \min[v'_k(t+1), d_k - 1]$.
3. Randomization. For all vehicles, if $v_k > 0$, the speed of the vehicle is decreased randomly by unity with probability p_{dec} to obtain the speed of next time step, i.e., $v_k(t+1) = \max[v''_k(t+1), 0]$ if rand() $< p_{\text{dec}}$, where rand() denotes a random number uniformly distributed from 0 to 1.
4. Movement. $r_k(t+1) = r_k(t) + v_k(t+1)$.

To apply NaSch model to multilane traffic, it should be generalized by adding the rules of lane changing. And the whole process can be divided into two parts: lane changing at first and the original single-lane update after lane changing. As for the rules of lane-changing, several previous studies have investigated this theme [11, 12, 20]. Rickert et al. [20] has proposed the following rules: If the position of car k is r_k, and car l and m are cars on the other lane such that $r_l \leq r_k < r_m$ and that there is no car between l and j. (The quantity $r_k - r_l$ is "the headway on the other lane".) Then car k will chang lane if:

1. Empty cells in front of the car on the current lane is small: $d_k - 1 < l_{\text{front},k} = \min(v_k + 1, v_{max})$.
2. More empty cells exist on the lane beside: $r_m - r_k > l_{\text{front},k} + 1$.
3. The gap between the car and the car behind it on the other lane is large: $r_k - r_l > l_{\text{back},k} = v_{max} + 1$.
4. A stochastic factor: rand() $< p_{\text{change}}$.

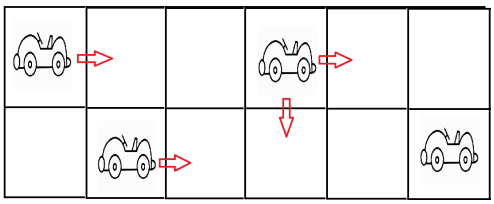

FIG. 1. An illustration of two-lane traffic on the lattice

Applying this generalized NaSch model to two-lane traffic, numerical simulation can show how the number of cars on two lanes will change with time (see FIG. 2).

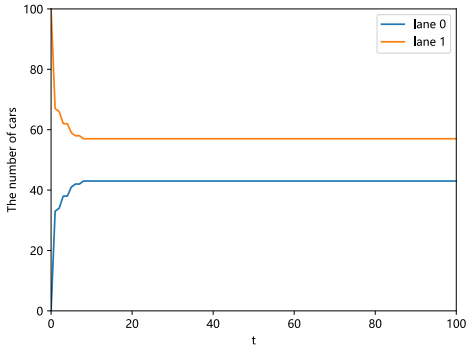

FIG. 2. The number evolution of cars under Rickert's rules. The result is produced under the condition that $p_{\text{change}=1}$, $v_{\max} = 2$, the lattice length l_0 is 200, the initial car density on lane 0 is 0 and on lane 1 is 0.5.

This picture indicates that if no car exist on one lane at the beginning, the exchange of cars between the two lanes will end after only a few steps without obtaining two lanes with equal number of cars, because of the strict requirement of Rickert's lane-changing rules. This is far from the real situation on the roads because people will change lane even if the number of cars on the other road is obviously less than the current one.

Since we will be studying the "blocking by slow car" case where lane changing is important, we modify the rules to exaggerate changing frequency a little. We use the same form of changing rules as Rickert's rule, but set $l_{\text{front},k} = d_k$, $l_{\text{back}} = 0$ and change the second rule into $r_m - r_k > l_{\text{front},k}$. It means a car will change lane (up to a stochastic factor) whenever more empty cells exist in front on the other lane and the cell right beside the car is empty. The evolution of the number of the cars on two lanes is shown in FIG. 3. The exchange of cars between the two lanes will take a while. Finally the number of cars on the two roads becomes close to each other and reaches a stable state. This is closer to the case in reality. Moreover, the number of cars at an interested time generally does not depend on the initial density ratio of the two lanes, and in all calculations below, the initial density of the two lanes are set to be equal.

PBC is taken, as has been mentioned, throughout this work for convenience. However, to make the system with PBC a good analog to a segment of a high way with entrance and exit of cars, the total number of time steps cannot be extended to infinity, and is limited to several hundreds of steps. Meanwhile, since the stochastic factor p_{change} and p_{dec} will complicate the model, it will be fixed at 1 until we investigate the influence of p_{change} in section VI. In practice, such case corresponds to ideal auto-pilot vehicles.

Furthermore, in order to simulate the difference of cars on the road (e.g., private cars, vans or buses), inhomogeneity of cars is introduced in our model. The $v_{\max}$'s of cars are set to be different. Two different kinds of cars are considered: $v_{\max,s}$ for slow cars and $v_{\max,f}$ for fast cars. The proportion of slow cars are denoted by P_{slow} here and after. To the best of our knowl-

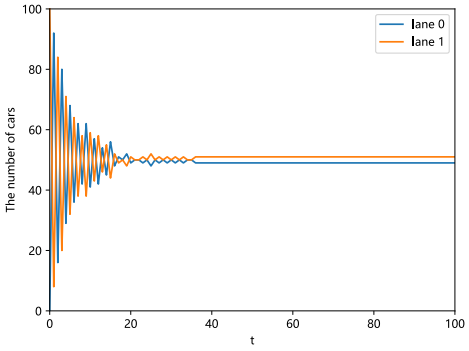

FIG. 3. The number evolution of cars under modified lane-changing rules. The result is produced under the condition that $p_{\text{change}} = 1$, $v_{\max} = 2$, the lattice length l_0 is 200, the initial car density on lane0 is 0 and on lane1 is 0.5.

edge, it is possibly the first time when the two-lane model and inhomogeneous-car model are combined in one study.

III. QUALITATIVE DESCRIPTION

In this section, various phenomena and different phases of the generalized NaSch model defined in the last section will be qualitatively analyzed.

Several simulations were conducted under different density ρ with P_{slow} remain fixed at 0.1. Each simulation is started from a random configuration with random vehicular speed. Typical spatial-temporal evolution diagrams are given in FIG. 4. Only the evolution of one lane is presented here due to symmetry. Three different phases of the model are found.

When ρ is low, as is mentioned before, cars are able to change lanes to overtake the leading cars of the high-density regions and enter the low-density regions (FIG. 4a). We call this phase the free fast car (FF) phase. (In some articles, the abbreviation "FF" may be used for other meanings, but we stick to this name and the reader should not confuse our definition with other research.) Note that lane changing is possible only if the region *beside* a car (on the other lane) is empty enough.

As the density increases on both lanes, lane changing becomes increasingly difficult. Finally, if the region beside a car in a high-density region is also high-density, lane changing stops and overtaking becomes impossible. Then, no car is able to enter the low-density regions. Since the leading slow car moves at its maximum speed $v_{\max,s}$, all cars queuing up behind it move at this speed as a whole (FIG. 4b), thus leading to the formation of platoons and vacancies. This phase is called the Bose-Einstein-like Condensation (BEC) phase. The reason for this analogy will be given in detail in section VI. It is characterized by the existence of platoons and vacancies. It is worth noticing that although local density is high in the platoon, empty cells still exist between cars. Otherwise the cars will stop due to the rule of the model.

The third phase occurs at high density. If ρ is increased in the BEC phase, one may expect that the total platoon length may grow due to increased number if cars. Eventually, the platoons on one lane touch each other and vacancies cease to exist. It marks the appearance of the third phase, which we call the high-density congested (HC) phase (FIG. 4c). If density is increased further, some highly-congested regions may appear, in which cars become so close that no empty cells exist, and thus the cars stop. These highly-congested regions lead to the the dark black lines in FIG. 4c, which characterizes the HC phase. It can be seen from the figure that, these dark lines, or the highly-congested regions move backward relative to the traffic flow at constant speed, which is in good agreement with previous results mentioned in [1].

To end this section, it is illuminating to compare the evolution of our multilane model with the original single-lane model. Two simulations with lane changing turned off is shown in FIG. 5. FIG. 5a and FIG. 4a were run under the same ρ and P_{slow}. The single-lane system quickly relaxes from the random initial configuration to a BEC phase without a lasting FF phase. It is natural because cars will always be blocked in a single lane as long as one slow car exists. Therefore, it can be concluded that the FF phase is peculiar to our multilane model.

IV. PHASE DIAGRAM OF THE MODEL

Based on the qualitative observation in the last section, it is tempting to obtain the phase diagram of our model in the (ρ, P_{slow}) space. To quantitatively distinguish the three phases, there should be a quantity behaving differently in the three phases. We have found the mean speed $\bar{v}$ of all cars in the system such a quantity. For clarity, $\overline{(\cdot)}$ is used to denote the mean quantity of all cars in *one* configuration, and $\langle\cdot\rangle$ is used to denote the *ensemble* average of a quantity.

The value of $\bar{v}$ at different P_{slow} and ρ is calculated and is given in FIG. 6, indicating how $\bar{v}$ distinguishes the three phases. In the FF phase, the mean speed is greater than the maximum speed of slow cars because fast cars may overtake the slow cars. As ρ increases, the increasing difficulty of lane changing leads to the decrease of $\bar{v}$. In the BEC phase, all cars fall into platoons and is blocked by a leading slow car. All cars move at the same speed, the maximum speed of slow car $v_{\max,s}$ (the platform in FIG. 6b). In the HC phase, the speed is limited by high density. Thus, $\bar{v}$ is less than $v_{\max,s}$ and decreases as the road becomes more congested with a greater ρ. In conclusion, for one definite configuration i (where the position and speed of all vehicles are known) with a definite $\bar{v}(i)$, the *configuration* i is in one of the three phases:

1. the FF phase if $\bar{v}(i) > v_{\max,s}$,
2. the BEC phase if $\bar{v}(i) = v_{\max,s}$, or
3. the HC phase if $\bar{v}(i) < v_{\max,s}$.

Additionally, it is worth mentioning that $\bar{v}$ depends on P_{slow} only in the FF phase. In the BEC phase, all cars move at $v_{\max,s}$, naturally independent of P_{slow}. In the HC phase, the distance between cars is smaller than $v_{\max,s}$, and the dynamics in the HC

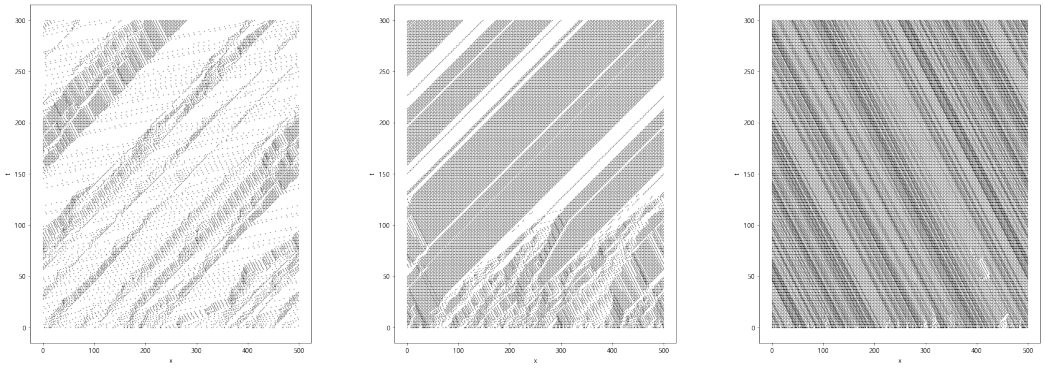

(a) (b) (c)

FIG. 4. Spatial-temporal evolution of the three phases in the multilane model. The horizontal axis represent the position on the lane and the vertical axis marks the time evolution. (a) ($\rho = 0.1,\ P_{\text{slow}} = 0.1$): The FF phase, where fast cars are able to overtake slow cars. (b) ($\rho = 0.25,\ P_{slow} = 0.1$): The BEC phase, where platoons and vacancies are formed and all cars move at the maximum speed of slow cars. (c) ($\rho = 0.5,\ P_{\text{slow}} = 0.1$) The HC phase, where vacancies disappear and high-density congested regions (the dark lines) appear. All calculations are performed under the lattice length $l_0 = 500$, $v_{\text{max,s}} = 2$ and $v_{\text{max,s}} = 10$. All stochastic factors turned off.

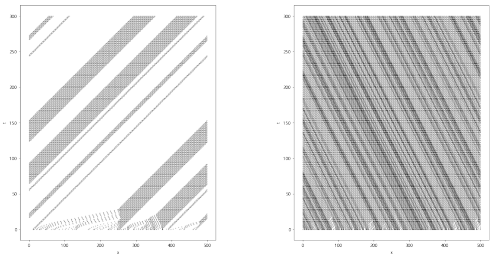

(a) (b)

FIG. 5. Spatial-temporal evolution of the single-lane model. (a) ($\rho = 0.1, P_{\text{slow}} = 0.1$): The BEC phase. No lasting FF phase exists here. (b) ($\rho = 0.5, P_{\text{slow}} = 0.1$): The HC phase. Other conditions are the same as the multilane model.

phase is thus almost completely determined by the rule $v_k = d_k - 1$, where d_k is the headway. Thus, v_{max} does not affect the dynamics here, and fast cars become indistinguishable from slow cars. Actually, the relationship $\bar{v}(\rho)$ in the HC phase can be determined with the preceding arguments:

$$\bar{v}(\rho) = \overline{d-1} = \frac{1}{N}\sum_{k=1}^{N} d_k - 1 = \frac{l_0}{N} - 1 = \frac{1}{\rho} - 1, \quad (1)$$

where d_k is the headway of car k and ρ is the density. It is the same as the situation in single-lane traffic [9]. Some validation of Eq. 1 is provided in appendix A. In contrast, in the FF phase, the distinction between fast and slow cars becomes significant due to overtaking, and $\bar{v}$ strongly depends on P_{slow}.

Though the criterion of a configuration's phase has been obtained above, we define another concept, the "time-dependent ensemble-averaged phase" to depict the phase diagram. We define the average phase of the *system* (instead of a configuration) at time t as:

1. the (averaged) FF phase, if $\langle \bar{v}_t \rangle > v_{\text{max,s}} + \delta_2$,
2. the (averaged) BEC phase, if $v_{\text{max,s}} - \delta_1 \le \langle \bar{v}_t \rangle \le v_{\text{max,s}} + \delta_2$, or
3. the (averaged) HC phase, if $\langle \bar{v}_t \rangle < v_{\text{max,s}} - \delta_1$,

where δ_1 and δ_2 is up to choice, and $\langle \bar{v}_t \rangle$ is the ensemble average of $\bar{v}_t$. The exact value of $\langle \bar{v}_t \rangle$ is defined as the following: Suppose there are M possible initial configurations in total. Let the system start from an initial configuration i, and let it evolve to get the configuration at time t, denoted by $j_{t,i}$. If the mean speed of cars of configuration $j_{t,i}$ is $\bar{v}(j_{t,i})$, then the exact ensemble average is defined as the average over different initial configuration i's:

$$\langle \bar{v}_t \rangle = \frac{1}{M}\sum_{i} \bar{v}(j_{t,i}). \quad (2)$$

Note that this definition only works when the stochastic factor has been turned off.

Such definition is due to two reasons. First, we introduce the time dependence because we are interested in the time evolution of phases of the system. For example, the system may exhibits the FF phase immediately after the initial configuration, and gradually evolves to the BEC phase. Furthermore, the concept of "steady phase" is far from reality. We have found that it sometimes takes a drastically long time (e.g., thousands of steps) to reach another phase. As is mentioned in section IV, the model is able to work as an idealization of the real

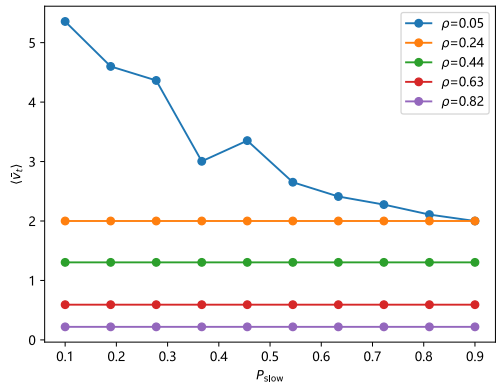

(a)

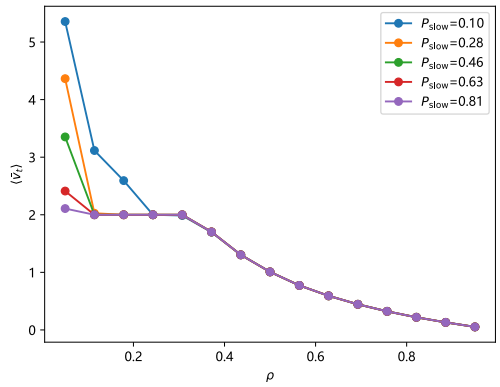

(b)

FIG. 6. The relationship between $\langle \bar{v}_t \rangle$ and ρ, P_{slow}. (a): $\bar{v}$ does not depends on P_{slow} except in the FF phase. (b): The graph consist of three parts signifying three phases. All calculations are performed under $l_0 = 500$, $v_{\text{max,s}} = 2$, $v_{\text{max,f}} = 10$ and at time time step $t = 200$. The average of 5 ensembles is taken.

traffic only in a finite range of time, and the phase reached after thousands of steps, for all practical reasons, is of no interest to us.

The second reason is that we want to incorporate different initial configurations into the phase diagram so that the phase diagram works as a property of the traffic system (under our model) generally. This incorporation is essential because a segment of the high way may be in all kinds of configurations when an observation starts. The time-dependent phase diagram should, in principle, predicts what phase the segment will be in after a certain time, based only on the parameters (ρ, P_{slow}) without detailed knowledge of the initial configuration. The randomness of the initial configuration will naturally lead to the indeterminacy of the prediction, i.e., one (ρ, P_{slow}) corresponds not to a unique phase after a certain time, but a probability distribution in the three phases. However, we found from simulations that for most values of (ρ, P_{slow}), one phase would dominate (possibly except at the phase borders). Thus, we introduce the concept of ensemble average into the definition, and δ_1 and δ_2 is introduced to deal with fluctuations.

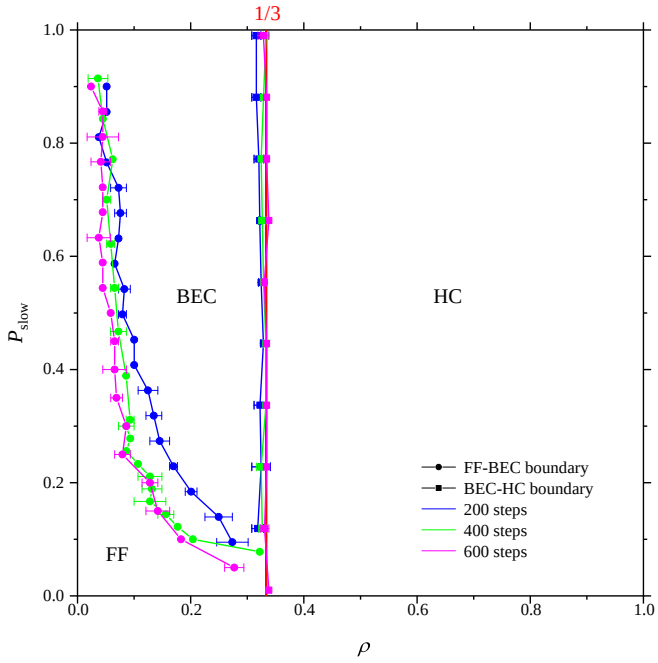

FIG. 7. The (average) phase diagram of the model at different time steps. The error bar in the diagram is due to the fluctuations at the border. A a red solid line marking the exact value $\rho = 1/3$ and is covered by the three BEC-HC boundaries. Note that points falling on the intersection of two boundaries haven't been calculated and are not shown in the diagram. All calculations are performed at $l_0 = 500$, $v_{\text{max,s}} = 2$, $v_{\text{max,f}} = 10$ and the average of 5 ensembles is taken.

The phase diagram, under the definition explained above, is given in FIG. 7. For our purposes, $\delta_1 = 0.001$ and $\delta_2 = 0.01$ is chosen based on the magnitude of fluctuations. In practice, taking all possible initial states into consideration is difficult, and we sample only a small proportion of all initial states (5 samples), which suffices to reveal the nature of the system.

Some further analysis can be given. First, the HC-BEC border can be solved with simple arguments. In the BEC phase, all platoons move at the speed $v_{\text{max,s}}$. Thus, the number of empty sites in front of each car in the platoon must be precisely $v_{\text{max,s}}$ according to rule of the model. The headway is thus $d_k = v_{\text{max,s}} + 1$. Only the headway of leading cars are different from it and may be much greater. In one of the extreme cases, we expect that there is only one huge platoon of length l_0 moving at $v_{\text{max,s}}$ with all cars possessing the same headway. Any increase of density will decrease $\bar{v}$ and drive the system into the HC phase. Thus, if the effect of lattice can be neglected, then the BEC-HC boundary is determined by

$$\sum_{k=1}^{N} d_k = N(v_{\text{max,s}} + 1) = l_0,$$

which means the BEC-HC critical density $\rho = N/l_0$ is given by

$$\rho_{\mathrm{BEC-HC}} = \frac{1}{v_{\mathrm{max,s}} + 1}. \tag{3}$$

It is equivalent to use Eq. 1 and let $\bar{v}(\rho_c) = v_{\mathrm{max,s}}$. In our simulation, $v_{\mathrm{max,s}} = 2$ and thus $\rho_{\mathrm{BEC-HC}} = 1/3$, which agrees perfectly with the numerical result.

Second, the time evolution of the phase diagram shown in FIG. 7 can be qualitatively analyzed. As time t increases, the FF-BEC border moves towards the lower left corner with a shrinking FF phase, while the BEC-HC border moves right and becomes closer to $1/3$. This phenomenon arises from the fact that it takes time for the formation of the BEC phase. When density is low, the system will be in the FF phase when t is relatively small, where the platoons are not completely formed and overtaking is still possible. When density is high, local high-density congested regions may exist due to random initial configuration and gradually release to form the BEC phase. Thus, the area between the 200-step BEC-HC border and the line $\rho = 1/3$ exhibits character of the HC phase, high-density congested regions, but these regions disappear as t increases. Furthermore, the difference between the 400-step diagram and the 600-step diagram is smaller than that of the 200-step and 400-step ones, which indicates the diagram may finally converge to a steady one. However, due to the practical reasons mentioned above, we stop our simulations at 600 steps to keep the model closer to reality.

In the following sections, we will study the features of the FF phase and the BEC phase in detail. Macroscopic quantities suitable for the description of each phase will be defined and investigated. Effects of lattice will be significant in the HC phase due to high density, and the model will not be a good approximation of real traffic. Thus, the HC phase will not studied in more detail, and the preceding discussion of $\bar{v}$ suffices to describe this phase in our model.

V. FEATURES OF THE FF PHASE

The FF phase is not a steady state due to lasting lane changing and is more chaotic than the BEC phase. Thus, entropy is a natural choice to describe the disorder of a configuration in the FF phase. The entropy of a configuration i in a single-lane traffic system has been defined in the context of information theory [21, 22] as:

$$S(i) = \sum_s P_s(i) \ln P_s(i), \tag{4}$$

where $P_s(i)$ is the proportion of cars in a *single-vehicle* state s in configuration i. In a single-lane traffic system, a single-vehicle state s is labeled by headway d_s and speed v_s. In other words, $P_s(i)$ is the proportion of cars possessing the same headway and speed (d_s, v_s) in the configuration i. Note that this information entropy is a quantity possessed by a configuration, and is defined through the statistics of cars in this configuration. However, in the mutlilane model, (d_s, v_s) cannot describe all the information of a single-vehicle state. Thus, we modify the single-vehicle state into (d_s, v_s, d'_s), where d'_s is the "headway on the other lane" used in the definition of lane changing rules (see section II).

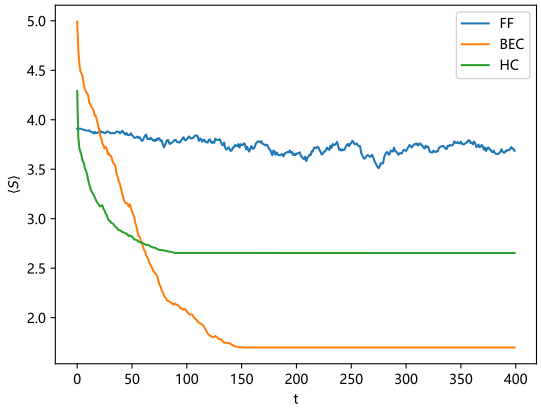

FIG. 8. The time evolution of the ensemble averaged $\langle S \rangle$. Fifty-ensemble average is taken.

The time evolution of the entropy (ensemble averaged) is calculated and is given in FIG. 8. It is evident that the entropy of the FF phase exhibits lasting fluctuation, while it reaches a steady value in the BEC or HC phase, which illustrates the unsteady nature of the FF phase. A time average of S will be used in the subsequent analysis due to this fluctuation. Note that a decrease in entropy appears before a steady state is reached in the BEC phase or the HC phase. It suggests that the traffic system self-organized to a more ordered configuration when relaxing from the random initial configuration.

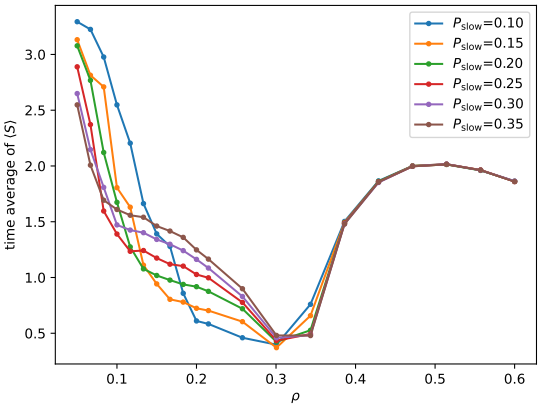

FIG. 9. The time average of the ensemble averaged $\langle S \rangle$ with respect to ρ is displayed. Fifty-ensemble average is taken

The time average of the entropy (ensemble averaged) is calculated and is given in FIG. 8. The distinct behavior of entropy in three phases could be recognized in the figure. In FF phase, sharp decrease of entropy occurs with the growth of ρ. The dis-

continuity of slope occurs when the system cross the FF-BEC boundary, which means the phase transition from FF to BEC is a *secondary* phase transition. In HC phase, the entropy is irrelevant with p_{slow}, which is in line with the analysis before.

As is mentioned above, entropy is useful in describing the degree of disorder in a system far from equilibrium state. From the phase diagram and qualitative description of FF phase (see section IV), we can infer the lane-changing behaviour of free fast cars is what cause the disorder of this phase. Therefore, the relation between car changing rate and entropy under different ρ and P_{slow} is investigated (FIG. 10). Here, the car changing rate is defined as the number of lane-changing cars over the total number of cars in one step.

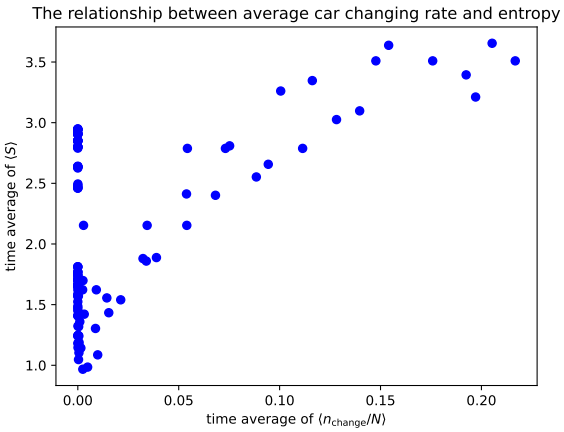

FIG. 10. The relation between car changing rate and entropy under different ρ and P_{slow}.

It can be inferred from FIG.10. that generally entropy and the car changing rate grows simultaneously. It is because the lane changing behaviour will change the headway and velocity of cars, thus raising the degree of disorder of the system. However, there are some points where entropy isn't zero while the car changing rate is zero. These points reside in the BEC phase, and the non-zero entropy is caused by the different distances between platoons. The distribution of cars obviously depends on the density ρ of cars and P_{slow}, which can be reflected by the difference of entropy in this case.

From all the analysis above, the lane-changing behaviour is a key factor in the FF phase. Therefore, we also take the possibility of lane-changing as a variable and study its relation with entropy. To ensure the validity of our modified model, the choice of P_{change} is between 0.8 to 1. From FIG. 11, entropy grows as P_{change} becomes bigger despite a local fluctation at $P_{\text{change}} = 0.84$.

VI. FEATURES OF THE BEC PHASE

The BEC phase will be studied in detail in this section. Previous studies have discovered similarity between platoon formation in single-lane traffic systems and Bose-Einstein Condensation [17, 18]. This analogy will be elaborated here. Con-

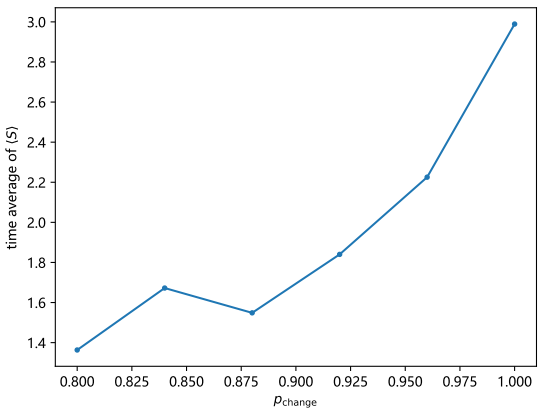

FIG. 11. The relation between car changing rate and entropy.

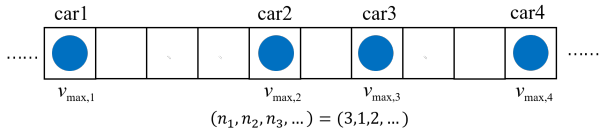

FIG. 12. An illustration of the BEC configuration. As an example, the state of the three empty sites in front of car 1 is defined as car 1.

sider a single-lane traffic model, there will be some lattices occupied by cars and some vacant ones. Due to translation invariance, a configuration can be written as car 1 followed by n_1 empty sites, car 2 followed by n_2 empty sites, etc. In other words, a configuration, or a microstate, can be denoted by $(n_1, n_2, \dots)$. If we regard the empty sites as Bosons, then the numbers $n_1, n_2, \dots$ are analogous to the occupation numbers of a state. Thus, the state of a Boson can be considered as the car immediately behind the Boson (see FIG. 12). Furthermore, the maximum speed of a car can be regarded as the energy value of the state defined by the car. Suppose all the cars possess different maximum speeds, and denote the car with the slowest maximum speed car 0. We will see that the slowest car is analogous to the ground state of the system. When the density is high, the lane is congested throughout, and the occupation number n_k of each state is low. This implies that each state contains only a small proportion of Bosons. Conversely, when the density decreases, vacancies and platoons emerge. Since all cars travel on one lane, they form a queue behind the slowest car 0, and a large vacant region emerges in front of car 0. Consequently, n_0 is high, and a significant proportion of Bosons condense on the state 0, It suggests that the slowest car is analogous to the ground state, and the platoon-forming phenomenon is analogous to BEC.

Slight difference exits in our model, and the definition of quantities describing this phenomenon should be taken with care. First, there are two lanes in our model. Second, there are only two kinds of cars and thus only two energy values: the slow cars correspond to the ground states, and the energy state

of the fast cars correspond to the high energy states. But numerous states, or cars, correspond to one energy value. However, we still apply the preceding analogy and label a configuration by $(n_1, n_2, \dots)$. As density decreases, Bosons (empty sites) will still condense to a few ground states, leading to several large n_k. The value of these large occupation number equals to length of vacancies. However, it is unclear which specific state (or car) the Bosons will condense on. In other words, which slow car will serve as a leading car is indeterminate. Thus, two quantities are defined to study the phenomenon. The first quantity is the maximum occupation number among $(n_1, n_2, \dots)$, denoted by $N_{0,\max}$. It is used to study the emergence of the BEC as density decreases. The second quantity is the average vacancy length $\bar{N}_0$. It is equal to the mean occupation number of states where a finite fraction of Bosons (empty sites) condense. This quantity is used to depict the character of the BEC phase. Meanwhile, the relationship of $N_{0,\max}$ with other quantities will be studied.

First, we study the dependence of $N_{0,\max}$ on different ρ, which is given in FIG. 13. In the BEC phase, low-energy-state vacancies decrease as the density grows and we can infer that macroscopically abundant particles condense on the low energy state. And once the system enters the HC phase, $N_{0,\max}$ is essentially $v_{\max,s}+1$ because no vacancy exists, which implies that no finite fraction of Bosons condenses on one state. This pattern is very similar to the behavior of the number of Bosons condensing on the ground state in BEC. Therefore, the analogy to Bose-Einstein-like condensation still works in the double-lane system here.

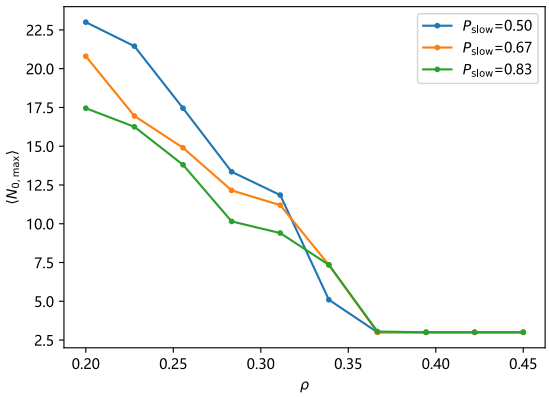

FIG. 13. The relationship between the ensemble averaged longest vacancy length $\langle N_{0,\max}\rangle$ and ρ. Twenty-ensemble average is taken.

The rest of this section will be dedicated to the investigation of the relationship of mean vacancy length $\bar{N}_0$ and other quantities. In our model, factors affecting the vacancy length mainly include: the proportion of the slow car P_{slow}, the density of cars ρ.

FIG .14 shows that the average vacancy length decreases as density grows. To further investigate this quantity, we may first hypythesis that all slow cars serve as a leading car. We call this situation the extreme BEC case. It can be inferred that the

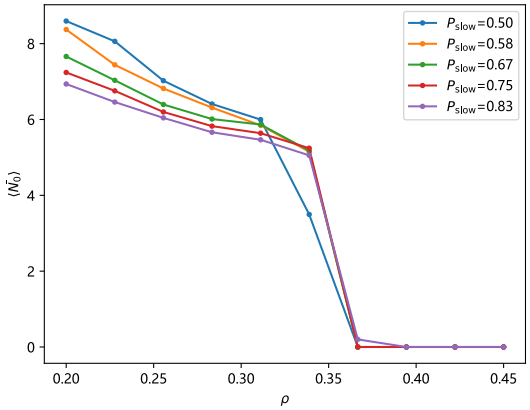

FIG. 14. The relationship between the ensemble averaged average vacancy length $\langle \bar{N}_0 \rangle$ and ρ. Twenty-ensemble average is taken. The average vacancy length $\bar{N}_0$ is defined to be 0 in the HC phase because no macroscopic vacancy appears.

average vacancy length $\bar{N}_0$, density ρ and P_{slow} satisfy:

$$\bar{N}_0 = \frac{1}{\rho P_{\text{slow}}} - \frac{v_{\max+1}}{P_{\text{slow}}} + v_{\max} \tag{5}$$

From the above equation, the average vacancy length should be inversely proportional to ρ, which is different from what FIG. 14. shows. Therefore, it can be inferred that not all the slow cars serve as a leading car. Instead, some of them will be in the middle of a platoon, the number of which is defined as the degeneracy of slow cars. Total degeneracy could reflect how the condensation in numerical simulation differs from the extreme BEC case. However, despite the physical picture of the quantity $\bar{N}_0$, the average platoon length $\overline{L}$ is more convenient for investigation. Recall that a platoon is the region where cars queue up behind a leading slow car. The investigation of $\overline{L}$ is equivalent to $\bar{N}_0$ due to symmetry. In the extreme BEC case, the average platoon length is:

$$\overline{L} = \frac{1}{\rho P_{\text{slow}}} - \bar{N}_0 = \frac{v_{\max,s}+1}{P_{\text{slow}}} - v_{\max}. \tag{6}$$

To investigate how $\overline{L}$ deviates from the extreme case, $\overline{L}$ is calculated under different (ρ, P_{slow}), which is given in FIG. 15. Average platoon length $\overline{L}$ decreases with the growth of P_{slow}. It is because more platoons will form when there are more slow cars, but the total number of cars, and thus the total length of platoons remains unchanged. Therefore, the average platoon length will decrease as is predicted by the extreme case Eq. 6. Additionally, $\overline{L}$ grows with the increase of ρ due to increased car numbers as expected, but significant nonlinear behavior exists.

We attempt to give a phenomenological correction to the extreme BEC case (Eq. 6) through the quantitative analysis of the total degeneracy of slow cars, denoted by α. To avoid cumbersomeness, we here denote the number of slow cars as

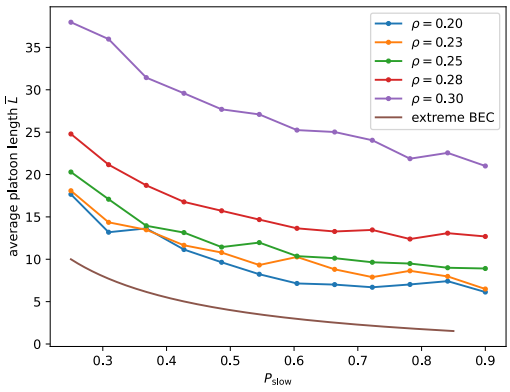

(a)

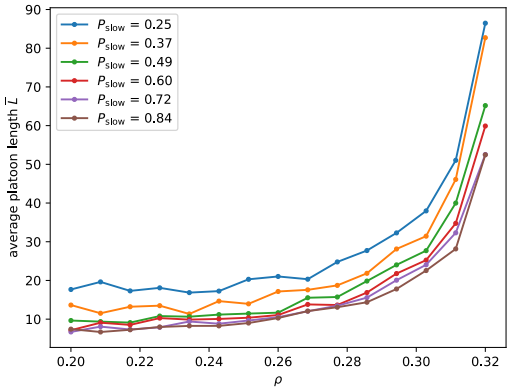

(b)

FIG. 15. (a) describes how average platoon length are correlated with the proportion of the slow car, under different ρ. The numerical value is greater than the extreme BEC case because not all slow cars serve as a leading car. (b) describes the relationship of average platoon length and ρ. The range of ρ is chosen to keep the system in the BEC phase. These figures are obtained with time step 400 and lattice length $l_0 = 500$. Each dot's value is the average of 50 ensembles.

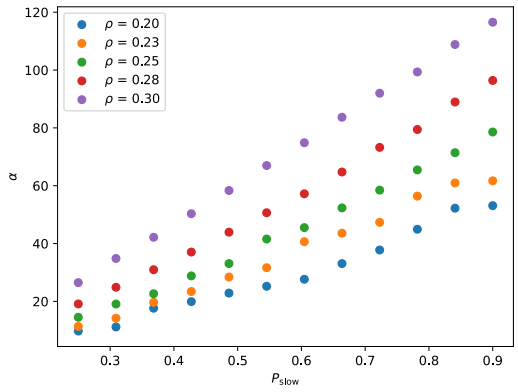

(a)

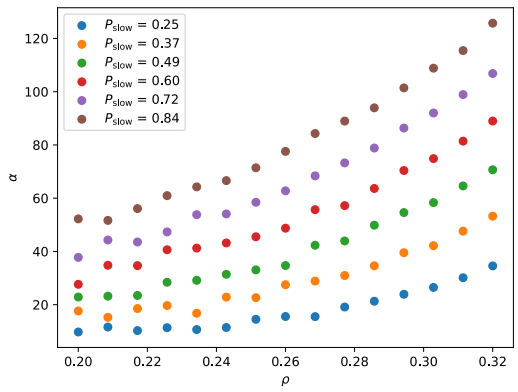

(b)

FIG. 16. (a): The relationship between total slow car degeneracy α and P_s. A linear regression is carried out under each ρ, where r value is no less than 0.98. (b) A numerical calculation of the relationship between α and ρ. These figures are again obtained with time step 400 and lattice length $l_0 = 500$.

n_s, the fast car n_f, the number of leading cars n_l, the length of the road l_0, the proportion of slow car P_s, the maximum speed of slow cars $v_{m,s}$, and the density ρ. The degeneracy α is then

$$\alpha = n_s - n_l, \tag{7}$$

which symbols the number of slow cars participating in the platoon while not serving as the leading car. In the extreme BEC case, all slow cars are assumed to be a leading car, which leads to the factor P_{slow} in the denominator of Eq. 6. A non-zero α suggests a decrease in the number of leading cars, whichs result in an effective P'_{slow}. Straightforward calculation gives

$$\alpha(P_s, \rho) = l_0 \rho \left(P_s - f(P_s, \rho)\right), \tag{8}$$

where

$$f(P_s, \rho) = \frac{v_{m,s} + 1}{\bar{L}(P_s, \rho) + v_{m,s}}. \tag{9}$$

The relationship $\alpha(\rho, P_s)$ is given in FIG. 16. It can be concluded from FIG. 16a that the relationship between α and P_s is approximately linear. We carry out a linear regression for each $\alpha(P_s)$. Note that the slope and the intersection of the α-P_s line depends on ρ.

To further derive a correction for $\bar{L}$, the dependence of the slope $\partial\alpha/\partial P_s$ on ρ is calculated and is given in FIG. 17. The relationship between $\partial\alpha/\partial P_s$ and ρ is approximately linear, which gives

$$\frac{\partial \alpha}{\partial P_s} = k_0 \rho + b_0, \tag{10}$$

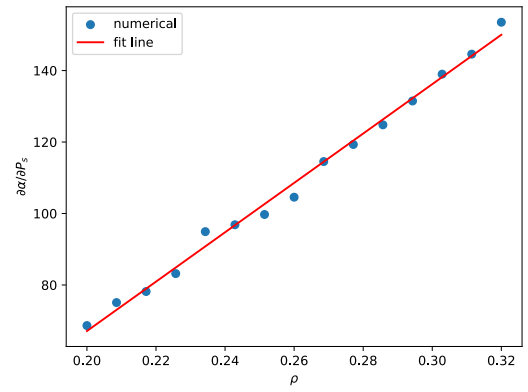

(a)

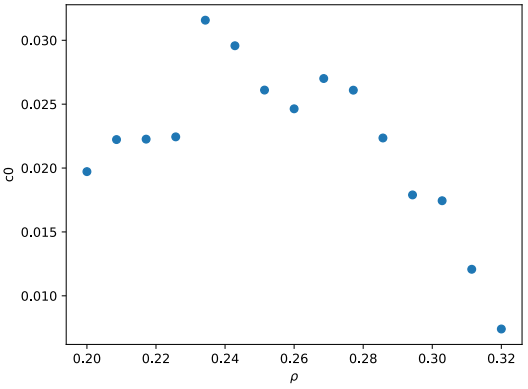

(b)

FIG. 17. (a): The relationship between the α-P_s slope and ρ. A linear regression gives an $r = 0.997$ (b) The relationship between c_0 and ρ, where $-c_0 l_0$ is the intercept of the α-P_s fit line. Calculations are carried out with time step 400 and lattice length $l_0 = 500$.

and

$$\alpha = (k_0\rho + b_0)P_s - c_0 l_0, \tag{11}$$

where c_0 can be obtained through the intercept of the α-P_s fit line (see FIG. 17b). Such a phenomenological relationship would tell us the exact relation of the f on P_s in Eq. 8, from which a correction of $\overline{L}$ can be given:

$$\overline{L} = -v_{m,s} + \frac{v_{m,s}+1}{\left[1 - \frac{1}{l_0}\left(k_0 + \frac{b_0}{\rho}\right)\right]P_s + \frac{c_0(\rho)}{\rho}}. \tag{12}$$

Eq. 12 serves as a phenomenological correction of the extreme BEC case Eq. 6. The relationship of $\bar{L}$ and P_s is plotted in FIG. 18. It fits the numerical value far better than the BEC case. Despite the corrected dependence of $\bar{L}$ on P_s, non-trivial behavior of $c_0(\rho)$ occurs when P_s increases, and a close form of the dependence of $\overline{L}$ and ρ still requires further study. At this stage, we are only able to use the numerical value of $c_0(\rho)$ to give the result in FIG. 18.

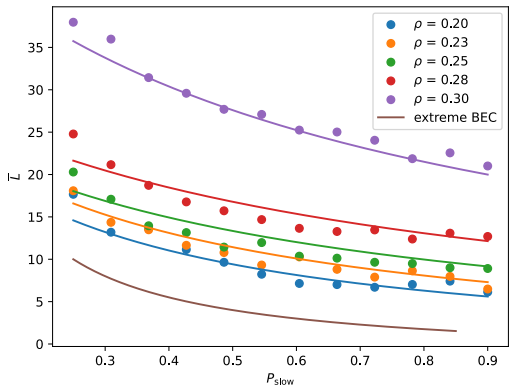

FIG. 18. A comparison of the phenomenological relationship $L(P_s)$ and numerical calculation. The dots are numerical calculation identical to FIG. 15a. The solid lines are the corrected relationships obtained in Eq. 12. The corrected relation fits the numerical values far better than the extreme BEC case. Note that the numerical values of $c_0(\rho)$ are used to plot the lines.

VII. CONCLUSION

This study is one of the first research focusing on the macroscopic properties of multilane traffic with inhomogeneous cars in a modified NaSch model.

We find that there are three different phases of cars when the density of cars and the proportion of slow cars differ. The phase diagram is given based on the characteristics of average velocity of different phases. Specifically, in the FF phase, overtaking is possible. In the BEC phase, all the cars "condenses" to the same velocity $v_{\max,s}$. In the HC phase, all the cars have velocity lower than $v_{\max,s}$.

Different quantities have been defined to make the description of these macroscopic phenomena more precise. In FF phase, entropy S is introduced.

In BEC phase, average vacancy or platoon length $\bar{L}_{\text{platoon}}$ and degeneracy are introduced.

Our study has extended previous studies on NaSch Model and Bose-Einstein-like condensation. The generalized NaSch model, in which the cars will change lane as long as there is space in front of it on another lane, is closer to reality and produces some new results compared with lane-changing rules in previous studies [11, 12, 20]. A new phase, the FF phase is found to occur when ρ and P_{slow} is low. With all the three phases, the different conditions of real road traffic can be more comprehensively described.

However, much work is left for future study. In terms of the model, other distributions of $v_{\max}$ (instead of only fast cars and small cars) can be used to model the traffic with greater accuracy. Additionally, the initial state sampled in the depiction of phase diagram can be more carefully chosen to approximate real situations. In terms of theory, the analysis of dynamics has to be developed in future to analytically obtain the phase diagram and the c_0 factor in the expression for average platoon

length.

VIII. ACKNOWLEDGES

We'd like to express our deepest gratitude for Professor Li Xiaopeng who offerred important instructions on our work. We are also thankful to our classmates for reading this article carefully and providing useful suggestions.

Appendix A: Fundamental Diagram

In this section, the flux of this system is defined, where the carrying capacity of different cars is taken into account. Subsequently, the fundamental diagram, namely the ρ-flux diagram, and P_{slow}-flux diagram, would be analyzed.

In order to describe the carrying capacity of the traffic system, a statistical quantity called *flux* is introduced, denoted by j.

The flux has been introduced in the NaSch Model with homogeneous cars, which is given by [9]:

$$j = \rho\bar{v}. \tag{A1}$$

The definition above only considers the flux of the cars, while neglecting the difference between the carrying capacity of different cars. Nevertheless, passenger-carrying capacity of cars could be a better measurement of a traffic system. Therefore, a weight factor for two different cars is introduced in order to define a reasonable flux of the system. The flux is now defined as

$$j = \rho\overline{\left(\frac{v}{v_{\max}}\right)}. \tag{A2}$$

The weight factor $1/v_{\max}$ is selected owing to two reasons. Firstly, we would like to exaggerate the capacity gap between two different kind of cars to illuminate the behavior of flux with respect to the change of the proportion of cars. In most of the settings we selected, the weight factor takes "1:5". Secondly, under this setup, the theoretical value of flux could be easily obtained. As a result, it would highlight the effect of congestion in the system.

From the fundamental diagram (FIG. 19b), several nontrivial phenomena occurs.

Firstly, the flux seems to converge to an identical value both at $\rho = 0.1$ and $\rho = 0.9$ regardless of the proportion of the slow car. Another fact is that flux seems to be linearly dependent on ρ in HC phase in FIG. 19a. Furthermore, from FIG. 19b and FIG. 19c, the flux of the system peaks around $\rho = 0.33$ regardless of P_{slow}, which is around the BEC-HC boundary. These nontrivial behaviors could be described by the analytical analysis below.

In the HC phase, all cars in the same system almost share the same speed regardless of the proportion of slow cars. Therefore, after neglecting the possible effect of non-continuous lattices, the flux satisfies

$$j_{\text{HC}} = \rho\bar{v}(\rho)\left(\frac{P_{\text{slow}}}{v_{\max,\text{s}}} + \frac{1-P_{\text{slow}}}{v_{\max,\text{f}}}\right), \tag{A3}$$

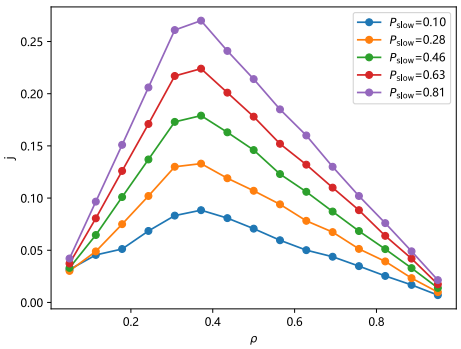

(a)

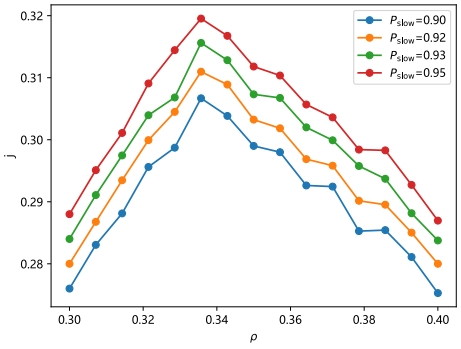

(b)

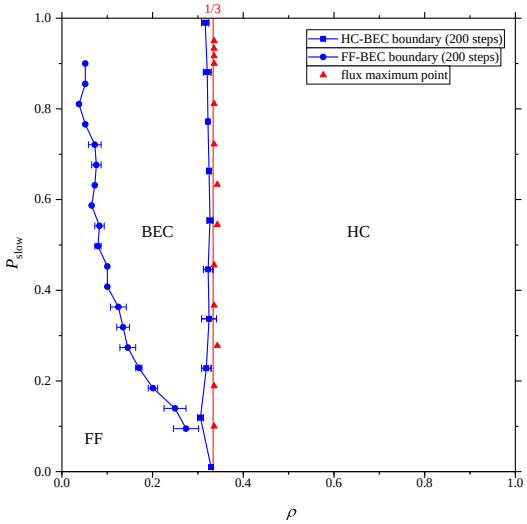

(c)

FIG. 19. Describes how flux is correlated with densityρ, under different P_{slow}. In FIG. 19a, 15 points were uniformly sampled for ρ from 0.1 to 0.9. In FIG 19b, 15 points were sampled uniformly around the peak of flux. Both the two figures are obtained under the condition that the time step is 200 and the lattice length l_0 is 500. Each dot's value is the average of 5 ensembles.

where $\bar{v}$ is the mean speed of cars, which depends only on ρ in HC phase, $v_{\max,s}$ is the maximum speed of slow cars, $v_{\max,f}$ is the maximum speed of fast cars and P_{slow} is the proportion of slow cars.

It is worth noticing that the contribution of ρ and P_{slow} in flux is factorized. Furthermore, the $\bar{v}(\rho)$ could also be determined by

$$\bar{v}(\rho) = \overline{d-1} = \frac{1}{N}\sum_{k=1}^{N} d_k - 1 = \frac{1}{\rho} - 1, \tag{A4}$$

where the meaning of the symbols are the same as Eq. A3.

It is the similar to the situation in single-lane traffic [9]. From Eq. A3 and Eq. A4, we could obtain

$$j_{\text{HC}} = (1-\rho)\left(\frac{P_{\text{slow}}}{v_{\max,s}} + \frac{1-P_{\text{slow}}}{v_{\max,f}}\right). \tag{A5}$$

The flux of BEC phase could also be determined by theoretical analysis. As the $\bar{v}$ remain unchanged in BEC phase, the flux of the system can be explicitly written in

$$j_{\text{BEC}} = \rho v_{\max,s}\left(\frac{P_{\text{slow}}}{v_{\max,s}} + \frac{1-P_{\text{slow}}}{v_{\max,f}}\right). \tag{A6}$$

With these analysis, the nontrivial behaviors mentioned above could be explained. Firstly, the reason for the convergence at low density limit is that fast cars and slow cars tend to decouple in the system at this limit. Meanwhile, two kinds of cars makes the equivalent contribution to the flux when they are free from interaction due to the setup of the flux. As a result, the influence of the proportion of the slow car would tends to vanish at $\rho \to 0$.

The reason for the convergence at high density limit is as follows. The contribution of ρ and P_{slow} in flux is factorized in Eq. A5. Namely, for a fixed ρ, the flux differs only up to a function of P_{slow}. At high density limit, $\bar{v}(\rho) \to 0$, so the flux tends to the same value.

Another point is that flux is linearly dependent on ρ in HC phase in FIG. 19a. The numerical result precisely matches the prediction of Eq.A5. For example, at $P_{\text{slow}} = 0.189$, the slope is given by $k_{\text{th}} = -0.1756$ from Eq. A5. Meanwhile, the slope obtained from numerical simulation is $k_{\text{ns}} = -0.174 \pm 0.001$. The prediction and the simulation result matches.

Thirdly , from FIG. 19b and FIG. 19c, the flux of the system peaks around $\rho = 0.33$ regardless of P_{slow}, which is around the BEC-HC boundary. It might be because the $\bar{v}$ remain unchanged in BEC phase. However, increasing ρ leads to increasing flux of the system.

Quantitatively, from Eq. A6, the flux is proportional to ρ. Thus, we expect the maximum flux to exist at the BEC-HC border, which is independent of P_{slow}. The reason why the flux maximum point resides a little right to the numerical HC-BEC border in FIG. 19 is that the result was obtained with time step $t = 200$, and, as is mentioned in section IV, local high-density congested regions haven't been fully released at $t = 200$, leading to a decreased $\bar{v}$ and a left-shifted BEC-HC border.

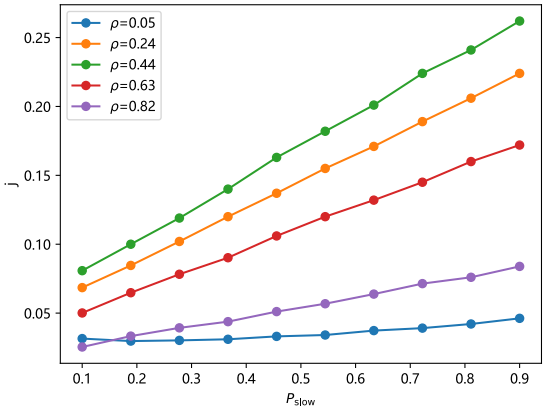

FIG. 20. Describe how flux is correlated with P_{slow},under different ρ. Ten points were uniformly sampled for P_{slow} from 0.1 to 0.9. The figure is obtained under the condition that the time step is 200 and the lattice length l_0 is 500. Each dot's value is the average of 5 ensembles.

To check the theoretical prediction, we analyzed the behavior of flux with respect to P_{slow} numerically (see FIG. 20). There is a very accurate linear increase in flux regarding P_{slow} at a fixed ρ except for $\rho = 0.05$.

It is because each j-P_{slow} curve would not cross the phase boundary as the BEC-HC boundary is independent of P_{slow}. Therefore, curves under different ρ satisfies either Eq. A5 or A6. Both equations are linear functions of P_{slow}, which matches the numerical result. However, for $\rho = 0.05$, the j-P_{slow} curve would cross the FF-BEC boundary at certain P_{slow}. As a result, nontrivial behaviors of flux occurs in FF phase when P_{slow} is small enough.

Appendix B: The determination of phase borders

Fluctuations appear close to the phase boundary because a dominate phase may fail to exist, in contrast to the bulk area of the phase diagram. In practice, according to the previous definition, we found out that the (average) phase of the system may switch between two phases close to the boundary due to fluctuations and limited number of calculations. Thus, we include error bars into the phase diagram, defined as the following.

To determine the phase border in FIG. 7, we scan the critical area of (ρ, P_{slow}) space with a fixed P_{slow} every time and varies ρ. For the FF-BEC border, 50 points for ρ from 0.01 to 0.35 and 20 points for P_{slow} are scanned, while more P_{slow} is scanned for the 400-step border due to fluctuations. For the BEC-HC border, 20 points for ρ from 0.295 to 0.375 and 10 points from 0.01 to 0.99 are scanned. For a point on the FF-BEC border, the left of the error bar is the first point that satisfies $v_{\max,s} - 0.001 \leq \langle \bar{v}_t \rangle \leq v_{\max,s} + 0.01$ and the right of the error bar is the first point to the right of which all points satisfy the condition for the BEC phase till the end of the scan. For a point on the BEC-HC border, the left of the error bar is

the first point that satisfies $\bar{v} < v_{\max,s} - 0.001$, and the right of the error bar is the first point satisfying the condition for HC to the right of which $\langle \bar{v}_t \rangle$ decreases monotonically with increasing ρ till the end of the scan. The diagram is given in FIG. 7. We have calculated the phase diagram at different time steps to study its time evolution.

Appendix C: Partition of work

All work has been separated into three equal parts, and it is not possible to explicitly list the partition of work. Generally speaking, literature review is separated into models, phenomena and thermodynamics (abolished later). Program development is separated into basic dynamics, lane-changing and BEC statistics. Calculation is separated into the phase diagram, the platoon length and the fundamental diagram. This completion of this article is separated into three equal parts. The score of the three authors have been discussed so that everyone claims $100/3$ points.

[1] D. Helbing, Traffic and related self-driven many-particle systems, Reviews of Modern Physics **73**, 1067 (2001).

[2] D. Chowdhury, L. Santen, and A. Schadschneider, Statistical physics of vehicular traffic and some related systems, Physics Reports **329**, 199 (2000).

[3] F. van Wageningen-Kessels, H. van Lint, K. Vuik, and S. Hoogendoorn, Genealogy of traffic flow models, EURO Journal on Transportation and Logistics **4**, 445 (2015).

[4] M. J. Lighthill and G. B. Whitham, On Kinematic Waves. II. A Theory of Traffic Flow on Long Crowded Roads, Proceedings of the Royal Society of London. Series A, Mathematical and Physical Sciences **229**, 317 (1955), 99769.

[5] B. S. Kerner and P. Konhäuser, Cluster effect in initially homogeneous traffic flow, Physical Review E **48**, R2335 (1993).

[6] I. Prigogine and F. C. Andrews, A Boltzmann-Like Approach for Traffic Flow, Operations research **8**, 789 (1960).

[7] L. A. Pipes, An Operational Analysis of Traffic Dynamics, Journal of Applied Physics **24**, 274 (1953).

[8] G. F. Newell, Nonlinear Effects in the Dynamics of Car Following, Operations research **9**, 209 (1961).

[9] B. Chopard, Cellular Automata Modeling of Physical Systems, in *Encyclopedia of Complexity and Systems Science*, edited by R. A. Meyers (Springer, New York, NY, 2009) pp. 865–892.

[10] K. Nagel and M. Schreckenberg, A cellular automaton model for freeway traffic, Journal de physique. I (Les Ulis) **2**, 2221 (1992).

[11] P. Wagner, K. Nagel, and D. E. Wolf, Realistic multi-lane traffic rules for cellular automata, Physica A: Statistical Mechanics and its Applications **234**, 687 (1997).

[12] K. Nagel, D. E. Wolf, P. Wagner, and P. Simon, Two-lane traffic rules for cellular automata: A systematic approach, Physical Review E **58**, 1425 (1998).

[13] Z. Zheng, Recent developments and research needs in modeling lane changing, Transportation Research Part B: Methodological **60**, 16 (2014).

[14] B. Tian, R. Jiang, M. Li, and M.-B. Hu, Cluster mean-field analysis for spontaneous symmetric breaking in a bidirectional two-lane system with narrow entrances and parallel update, Europhysics Letters **117**, 40003 (2017).

[15] Z. Ding, T. Liu, X. Lou, Z. Shen, K. Zhu, R. Jiang, B. Wang, and B. Chen, Mean-field analysis for Asymmetric Exclusion Processes on two parallel lattices with fully parallel dynamics, Physica A: Statistical Mechanics and its Applications **516**, 317 (2019).

[16] D. V. Ktitarev, D. Chowdhury, and D. E. Wolf, Stochastic traffic model with random deceleration probabilities: Queueing and power-law gap distribution, Journal of physics. A, Mathematical and general **30**, L221 (1997).

[17] M. R. Evans, Bose-Einstein condensation in disordered exclusion models and relation to traffic flow, Europhysics Letters **36**, 13 (1996).

[18] M. R. Evans, Exact steady states of disordered hopping particle models with parallel and ordered sequential dynamics, Journal of Physics A: Mathematical and General **30**, 5669 (1997).

[19] M. Schreckenberg, A. Schadschneider, K. Nagel, and N. Ito, engDiscrete stochastic models for traffic flow, Physical review. E, Statistical physics, plasmas, fluids, and related interdisciplinary topics **51**, 2939 (1995).

[20] M. Rickert, K. Nagel, M. Schreckenberg, and A. Latour, engTwo lane traffic simulations using cellular automata, Physica A **231**, 534 (1996).

[21] H. Reiss, A. D. Hammerich, and E. W. Montroll, Thermodynamic treatment of nonphysical systems: Formalism and an example (Single-lane traffic), Journal of Statistical Physics **42**, 647 (1986).

[22] A. Miura, A. Tomoeda, and K. Nishinari, Formularization of entropy and anticipation of metastable states using mutual information in one-dimensional traffic flow, Physica A: Statistical Mechanics and its Applications **560**, 125152 (2020).